Journal of Inflammation Research

Dovepress
Taylor & Francis Group

Open Access Full Text Article

ORIGINAL RESEARCH

The Role of Cuproptosis in Hyperoxia-Induced Lung Injury and Its Potential for Treatment

Kaihua Yu[1,*], Yunfei Gu[2,*], Ying Yao[1], Jianchun Li[3], Suheng Chen[1], Hong Guo[4], Yulan Li[5], Jian Liu[1,6]

[1]The First School of Clinical Medicine, Lanzhou University, Lanzhou, Gansu, People's Republic of China; [2]Anesthesiology Department, Gansu Provincial Maternity and Child-Care Hospital (Gansu Provincial Center Hospital), Lanzhou, Gansu, People's Republic of China; [3]Department of Intensive Care Unit, Suzhou Science and Technology City Hospital, Nanjing, Jiangsu, People's Republic of China; [4]Department of Anesthesiology, Inner Mongolia Hospital of Peking University Cancer Hospital, Hohhot, Inner Mongolia, People's Republic of China; [5]Department of Anesthesiology, First Hospital of Lanzhou University, Lanzhou, Gansu, People's Republic of China; [6]Gansu Provincial Maternity and Child-Care Hospital (Gansu Provincial Center Hospital), Lanzhou, Gansu, People's Republic of China

*These authors contributed equally to this work

Correspondence: Jian Liu; Yulan Li, Email medecinliujian@163.com; liyul@lzu.edu.cn

Video abstract

Point your SmartPhone at the code above. If you have a QR code reader the video abstract will appear. Or use: https://youtu.be/l-dcT3_dLv0

Background: Oxygen supplementation is essential for patients with a multitude of diseases but can cause severe hyperoxia-induced lung injury (HLI), necessitating the identification of therapeutic targets to improve clinical outcomes. Cuproptosis, a novel copper-dependent form of cell death characterized by proteotoxic stress resulting from lipoylated protein aggregation and loss of iron-sulfur cluster proteins, is distinct from other forms of cell death. However, the role of cuproptosis in HLI remains unclear.

Methods: We established an HLI model in MLE-12 cells and C57BL/6 mice to investigate the involvement of cuproptosis in hyperoxia-induced toxicity.

Results: We observed a time-dependent increase in the cuproptosis-related gene *Fdx1* under hyperoxia. Moreover, hyperoxia activated the membrane-associated copper transporter SLC31A1 and significantly elevated copper levels in MLE-12 cells, as well as in the serum and lung tissue of C57BL/6 mice. Further analysis revealed that hyperoxia significantly altered the expression of cuproptosis-related genes without affecting DLAT levels, but significantly increased lipoylated-DLAT levels. ELISA, CCK-8 assays, HE staining, lung wet-to-dry weight ratio, and bronchoalveolar lavage fluid analysis demonstrated that treatment with the cuproptosis inhibitor TTM reduced pro-inflammatory cytokines (TNF-α and IL-1β) and alleviated hyperoxia-induced injury in both MLE-12 cells and C57BL/6 mice.

Conclusion: Our study identifies the involvement of cuproptosis in HLI, providing new insights into the pathogenesis of hyperoxic lung injury and potential therapeutic strategies.

Keywords: hyperoxia, lung injury, hyperoxia-induced lung injury, cuproptosis, copper, FDX1

Introduction

Oxygen supplementation is a vital, life-saving therapy for patients with hypoxemia by enhancing arterial oxygen saturation.[1] However, prolonged exposure to high oxygen levels can cause severe hyperoxia-induced lung injury (HLI), a condition linked to postoperative pulmonary complications and prolonged hospitalization.[2] Oxygen participates in energy metabolism and is prone to forming reactive oxygen species (ROS), which can accumulate excessively and overwhelm cellular antioxidant defenses, leading to oxidative damage within cellular structures.[3,4] Despite years of research, the fundamental molecular mechanisms underlying HLI continue to be largely unknown, highlighting the need to identify key therapeutic targets for improving clinical outcomes. A comprehensive understanding of how hyperoxia induces lung injury is crucial for the effective management of patients requiring supplemental oxygen.

Type II alveolar epithelial cells are essential for maintaining the integrity of the pulmonary epithelium, serving as progenitor and immune cells involved in epithelial repair and regeneration.[5,6] Their dysfunction in response to various

Received: 14 December 2024
Accepted: 21 March 2025
Published: 3 April 2025

stimuli is closely associated with lung injury and represents a key target in HLI.[7] MLE-12 cells, derived from murine lung epithelium, are commonly used as a model for type II alveolar epithelial cells, providing a valuable system to investigate the mechanisms underlying HLI.

Copper plays a critical role as a cofactor for essential body enzymes, regulating various physiological processes.[8] Cuproptosis, a newly discovered form of copper-dependent cell death in 2022, is distinct from well-known pathways such as apoptosis, pyroptosis, autophagy, and ferroptosis. Its mechanism primarily involves copper ions binding to lipoylated components of the tricarboxylic acid (TCA) cycle through the FDX1-dependent pathway, leading to clustering of lipoylated proteins, depletion of Fe-S cluster-containing proteins, and induction of HSP70, indicative of acute proteotoxic stress.[9]

As early as 1998, a study showed that an excess of copper ions is closely associated with biological damage and oxidative stress.[10] Copper ions not only participate in Fenton-like reactions, promoting ROS generation, but also bind to the major intracellular antioxidant glutathione (GSH), diminishing the cellular antioxidant capacity,[11,12] which has been implicated in the potential exacerbation of HLI.[13] Cytochrome P450 (CYP) enzymes, a class of oxidases, can release ROS during the uncoupling steps of their reaction cycle, contributing to oxidative stress.[14] Adrenodoxin, encoded by *Fdx1*, plays a crucial role in this process by providing essential electrons to mitochondrial CYP enzymes, enhancing their catalytic activity.[15] The lack of CYP1B1 has been shown to mitigate the lung response to hyperoxia in adult mice.[16] Additionally, a study has indicated that hyperoxia may destabilize Fe-S cluster-containing proteins.[17] These findings collectively imply a potential involvement of cuproptosis in HLI development, yet its precise role and underlying mechanisms remain to be fully clarified.

In this study, we established an HLI model using MLE-12 cells and C57BL/6 mice and used the copper chelator TTM to investigate the role of cuproptosis in HLI pathogenesis. Hyperoxia exposure altered the expression of multiple cuproptosis-related genes, with notable increases in copper content, upregulation of the copper importer SLC31A1, and significantly elevated levels of FDX1 and lipoylated DLAT. These findings confirm the involvement of cuproptosis in HLI. Treatment with TTM effectively reduced hyperoxia-induced injury, suggesting that targeting cuproptosis may represent a promising therapeutic strategy for HLI prevention.

Materials and Methods

Cell Culture

The MLE-12 cell line, purchased from FuHeng Biology (China), was cultured in high-glucose DMEM (G4524, Servicebio) supplemented with 1% streptomycin-penicillin (G4003, Servicebio) and 10% fetal bovine serum (AB-FBS-1050, Abwbio). Cells were maintained at 37°C in a humidified incubator with 5% CO_2. Subconfluent cells were plated and allowed to adhere for 24 hours before treatment. Hyperoxia was induced by placing the cells in a sealed chamber with 95% O_2 and 5% CO_2, while control cells were cultured under normal conditions of 95% room air and 5% CO_2. The copper chelator tetrathiomolybdate (TTM) was purchased from Sigma-Aldrich. A stock solution of TTM was prepared using dimethyl sulfoxide (DMSO), and the final working solution, with a DMSO concentration below 0.01%, was applied to cells. Cells were pretreated with 4 μM of TTM for 30 minutes before exposure to hyperoxia or normoxia.

Treatment of Animals

Male C57BL/6 mice (6–8 weeks old, 15–18g) were purchased from Lanzhou University. All experiments were conducted following the Guidelines for the Ethical Review of Laboratory Animal Welfare of the People's Republic of China (GB/T 35892–2018) and were approved by the Animal Ethics Committee of the First Hospital of Lanzhou University (LDYYLL2024-210). Mice were randomly divided into four groups, with six mice per group (n = 6): Normoxia, Normoxia + TTM, Hyperoxia, and Hyperoxia + TTM. The Hyperoxia and Hyperoxia + TTM groups were exposed to hyperoxic conditions (85% O_2) in a sealed plexiglass chamber (22 °C, 50–70% humidity) for 7 days, while the Normoxia and Normoxia + TTM groups were kept in room air (21% O_2). Additionally, mice in the Hyperoxia + TTM group received 40 mg/kg of TTM via oral gavage once a day for 7 days. Mice in the Normoxia + TTM group received double-

distilled water containing 1.36% DMSO via oral gavage as a vehicle control. After 7 days of exposure, mice were euthanized, and blood, bronchoalveolar lavage fluid (BALF), and lung tissues were collected for further analysis.

Cell Viability Assessment

Cell viability was assessed utilizing the Cell Counting Kit-8 (CCK-8, G4103 Servicebio). MLE-12 cells were seeded at 1×10^5 cells per well in 96-well plates and treated with the designated agents for the specified durations. Following treatment, 100 μL of fresh medium along with 10 μL of CCK-8 solution were added to each well. The cells were then incubated in a 5% CO_2 incubator at 37°C for 2 hours. The absorbance at 450 nm was measured using a microplate reader (BioTek, SynergyH1).

Total Cells and Protein Concentration in BALF

After modeling, mice were anesthetized, and blood was collected via the abdominal aorta for euthanasia. The diaphragm was then incised to induce pneumothorax and expose the thoracic cavity. The trachea was exposed, and the left bronchus was ligated. Subsequently, 0.5 mL of PBS was instilled three times into the right lung and gently aspirated. The BALF was centrifuged, and the supernatant was collected for protein analysis using a BCA assay. The cell pellet was resuspended in 1 mL of PBS, mixed thoroughly, and the cells were counted.

Wet/Dry Lung Weight Ratio

The left lung tissue was collected and immediately weighed to obtain the wet weight. It was then dried at 60°C for 48 hours and reweighed to determine the dry weight. The wet/dry weight ratio was calculated.

Histopathology of Lung Tissue

The left lung tissue was fixed in 4% paraformaldehyde at room temperature for 24 hours. After dehydration, the tissue was embedded in paraffin and sectioned into 4 μm sections, which were stained with hematoxylin and eosin (H&E). Histopathological changes were assessed using optical microscopy. Quantitative analyses were performed using Image-Pro Plus 6.0, measuring the average linear intercept (MLI), radial alveolar count (RAC), and alveolar septal thickness (AST) in images with a 100 μm scale bar to assess alterations in alveolar size, number, and septal thickness. MLI estimates average alveolar size by dividing the total line length by the number of intercepts between alveolar walls. RAC evaluates alveolar structure by counting the number of alveoli along a radius from a respiratory bronchiole to the nearest connective tissue septum. AST measures the thickness of alveolar septa by assessing the distance between adjacent alveolar walls, helping to evaluate structural changes in the lung. Six tissue sections were selected from each group, and three fields of view were randomly chosen from each section for analysis.

Copper Content Detection

Copper content in cells was measured using the Cell Copper Colorimetric Assay Kit (E-BC-K775-M, Elabscience), and copper content in serum and lung tissue was assessed with the Copper Colorimetric Assay Kit (E-BC-K300-Me, Elabscience). All procedures were performed according to the kit instructions.

Enzyme-Linked Immunosorbent Assay (ELISA)

Levels of TNF-α and IL-1β in cells and BALF were measured according to the guidelines provided by the TNF-α (JL10484, Jonlnbio) and IL-1β (JL18442, Jonlnbio) ELISA kits.

RNA Extraction and Quantitative PCR

RNA was extracted using Trizol reagent, followed by reverse transcription with the PrimeScript™ RT Reagent Kit, which includes a gDNA Eraser (RR047A, Takara). Quantitative PCR (qPCR) was performed using TB Green Premix Ex Taq™ (RR820A, Takara) on the CFX96 Real-Time PCR Detection System (Bio-Rad). Relative gene expression was normalized to *β-actin* and calculated using the $2^{(-\Delta\Delta Ct)}$ method. Detailed information about the qPCR primers is provided in Table 1.

Table 1 The qPCR Primer Sequences

Targets	Forward 5′-3′	Reverse 5′-3′
Fdx1	ACAGACAGGAACCTGGAAGACC	GAGACAATCTGTATGGGGTGGTT
Lias	GCCGACGTGGACTGTTTAACTC	AAGATCGCACCAAAGGACCAC
Lipt1	AGAATCCGTGGCAGGAATGTAA	AAAGAAGGTGAGGTTGATGTTACCC
Dld	TAGAGAAGATGATGGAGCAGAAGCA	TTTGGTATCAATAACCTGAGTGCTG
Dlat	GTCTGAAAGTTCCCGAAGCAA	GGAGGCTAAAGAAACAACATCACT
Pdha1	ACCAGAGAGGATGGGCTCAAGT	AGGTGGTCCGTAGGGTTTATGC
Pdhb	AAGAAGTTGCCCAGTATGACGGT	GCTTGCATAGAGAAATTGAAGGTCA
Gls	AGTCTGGAGGGAAGGTTGCTG	GGGGTTTTACACAGGACTGAAGA
Mtf1	GGATGATGAAGACGATGGACAGT	CGCTTTACTTCTTTCCGTTTCG
Cdkn2a	GGTGATGATGATGGGCAACG	TCGCACGATGTCTTGATGTCC
Slc31a1	GTATGTCAACGCCATGCAC	GATGCCATTCATGAGTCTG
Atp7b	CCAGCATTCATCTCTCCAAGAGGAC	AAGAGACGAGAGCACCACAGAGACAG
Hsp70	CCGACAAGGAGGAGTTCGTG	ACAGTAATCGGTGCCCAAGC
β-Actin	AAATCTGGCACCACACCTTCTAC	CAGCCTGGATAGCAACGTACAT

Western Blotting Analysis

Cells and lung tissue were lysed for protein quantification, followed by separation and transfer of proteins to PVDF membranes. Membranes were incubated at 4°C overnight with primary antibodies: anti-DLAT (SAB, 1:1,000, #56637), anti-SLC31A1 (SAB, 1:1,000, #52861), anti-FDX1 (Abcam, 1:2,500, ab209809), anti-Lipoic Acid (Abcam, 1:3,000 ab58724), and anti-β-ACTIN (ABclonal, 1:50,000, AC038). Densitometric analysis of protein bands was performed using ImageJ2 software (version 2.9.0/1.53t), and the relative protein expression levels were normalized to β-ACTIN.

Statistical Analysis

All statistical analyses were conducted using GraphPad Prism 9 software. Data are presented as mean ± standard error of the mean (SEM). An unpaired *t*-test was used to compare two independent samples, while one-way ANOVA was employed for multiple group comparisons. Statistical significance was defined as $p < 0.05$.

Results

Hyperoxia Induces Injury and Increases Copper Content in MLE-12 Cells

To investigate the effect of hyperoxia on MLE-12 alveolar epithelial cells, we assessed cell proliferation under normoxic and hyperoxic conditions. Cells were cultured for 24, 48, and 72 hours, and proliferation was evaluated using CCK-8 assays (Figure 1A). The results indicated that hyperoxia significantly reduced cell proliferation compared to normoxia. To explore the potential role of copper in this process, we measured intracellular copper content (Figure 1B). Copper levels increased significantly under hyperoxia, peaking at 48 hours. Based on this, we selected 48 hours as the optimal time point for subsequent cell experiments. Additionally, to evaluate the impact of 48 hours of continuous hyperoxia exposure on MLE-12 cells, we measured the levels of inflammatory cytokines TNF-α and IL-1β in the cell culture supernatants using ELISA (Figure 1C and D). The results showed that hyperoxic stimulation significantly elevated these pro-inflammatory cytokines.

Copper Chelator Alleviates Hyperoxia-Induced Injury in MLE-12 Cells

To further explore the involvement of copper in hyperoxia-induced injury in MLE-12 cells, we used the copper chelator TTM. Pretreatment with the cuproptosis inhibitor TTM under hyperoxic conditions significantly enhanced cell proliferation (Figure 2A). Furthermore, compared to the normoxia group, copper levels in the hyperoxia group significantly decreased after TTM treatment, accompanied by a reduction in pro-inflammatory cytokine levels (Figure 2B–D). These findings suggest that the copper chelator can alleviate hyperoxia-induced cellular inflammation. Additionally, we assessed *Fdx1* mRNA expression using qRT-PCR and found a significant increase with prolonged hyperoxia exposure

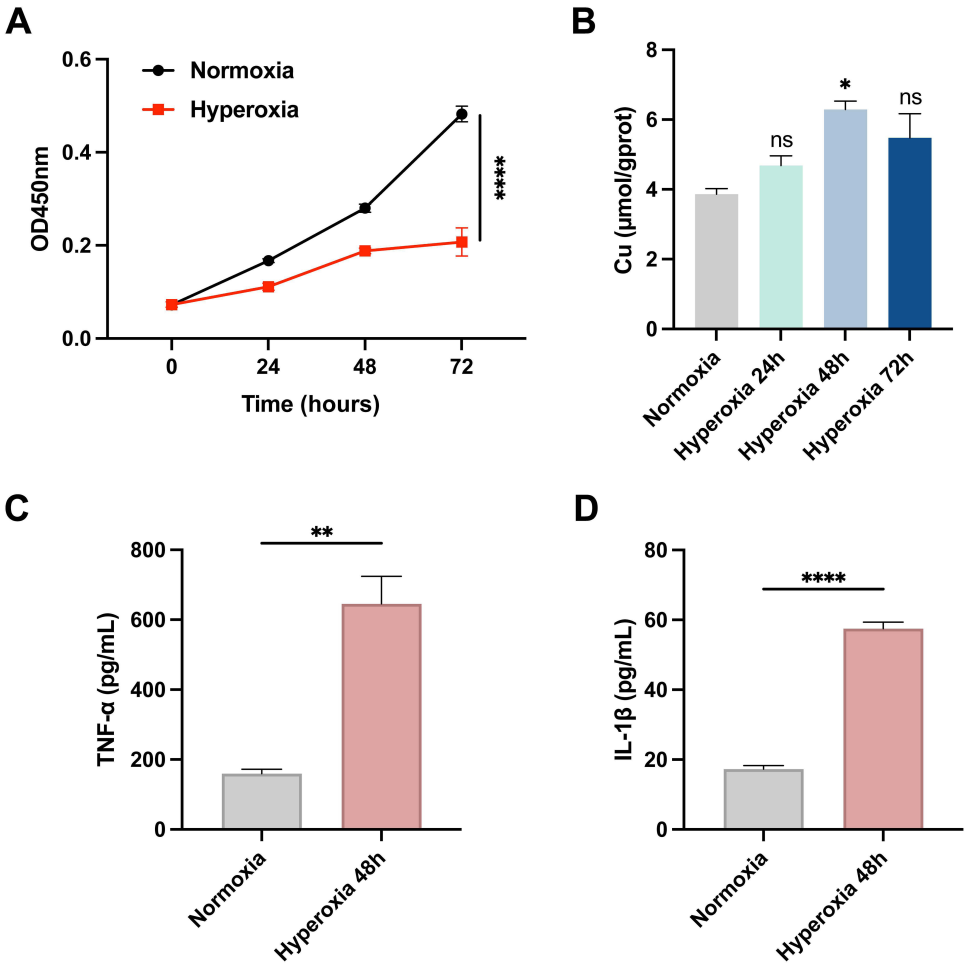

Figure 1 Hyperoxia exposure induces inflammatory responses and increases intracellular copper content in MLE-12 cells. (**A**) Cell proliferation quantified by CCK-8 assay. (**B**) Copper concentration within cells. (**C**) TNF-α levels in culture supernatants. (**D**) IL-1β levels in culture supernatants. The data were expressed as mean ± SEM, n = 3. **P*<0.05, ***P*<0.01, *****P*< 0.0001 versus normoxia group.

compared to normoxia (Figure 2E). The protein expression exhibited a similar trend, as demonstrated by Western blotting (Figure 2F and G), indicating that cuproptosis may be involved in hyperoxia-induced injury in MLE-12 cells.

Cuproptosis Involved in Hyperoxia-Induced Injury in MLE-12 Cells

To determine whether hyperoxia induces cuproptosis in MLE-12 cells, we assessed the expression of cuproptosis-related genes using qRT-PCR (Figure 3A–M). Under hyperoxic conditions, mRNA levels of *Fdx1, Lias, Lipt1, Dld, Gls, Mtf1, Cdkn2a, Slc31a1, Atp7b*, and *Hsp70* were significantly upregulated. In contrast, *Pdha1* and *Pdhb* were notably down-regulated compared to the normoxic controls. Pretreatment with TTM before the hyperoxia exposure effectively reversed these gene expression changes. At the protein level, FDX1 and SLC31A1 showed similar trends. Although hyperoxia did not affect *Dlat* mRNA and protein levels, it significantly increased the protein level of lipoylated-DLAT, which was markedly reduced by TTM pretreatment administered before hyperoxia exposure (Figure 3N and O).

Copper Chelator Alleviates Hyperoxia-Induced Lung Injury in Mice

To evaluate the protective effects of TTM on hyperoxia-induced lung injury in mice, multiple assessments were conducted. Histopathological examination of lung tissues using HE staining revealed significant lung injury, including alveolar hemorrhage, inflammatory cell infiltration, and thickened, edematous alveolar septa, after 7 days of hyperoxia exposure. In contrast, TTM treatment mitigated these injuries, resulting in less alveolar hemorrhage, decreased inflammatory infiltration, and attenuated alveolar edema (Figure 4A). Significantly higher MLI, AST, and RAC values were

https://doi.org/10.2147/JIR.S512187

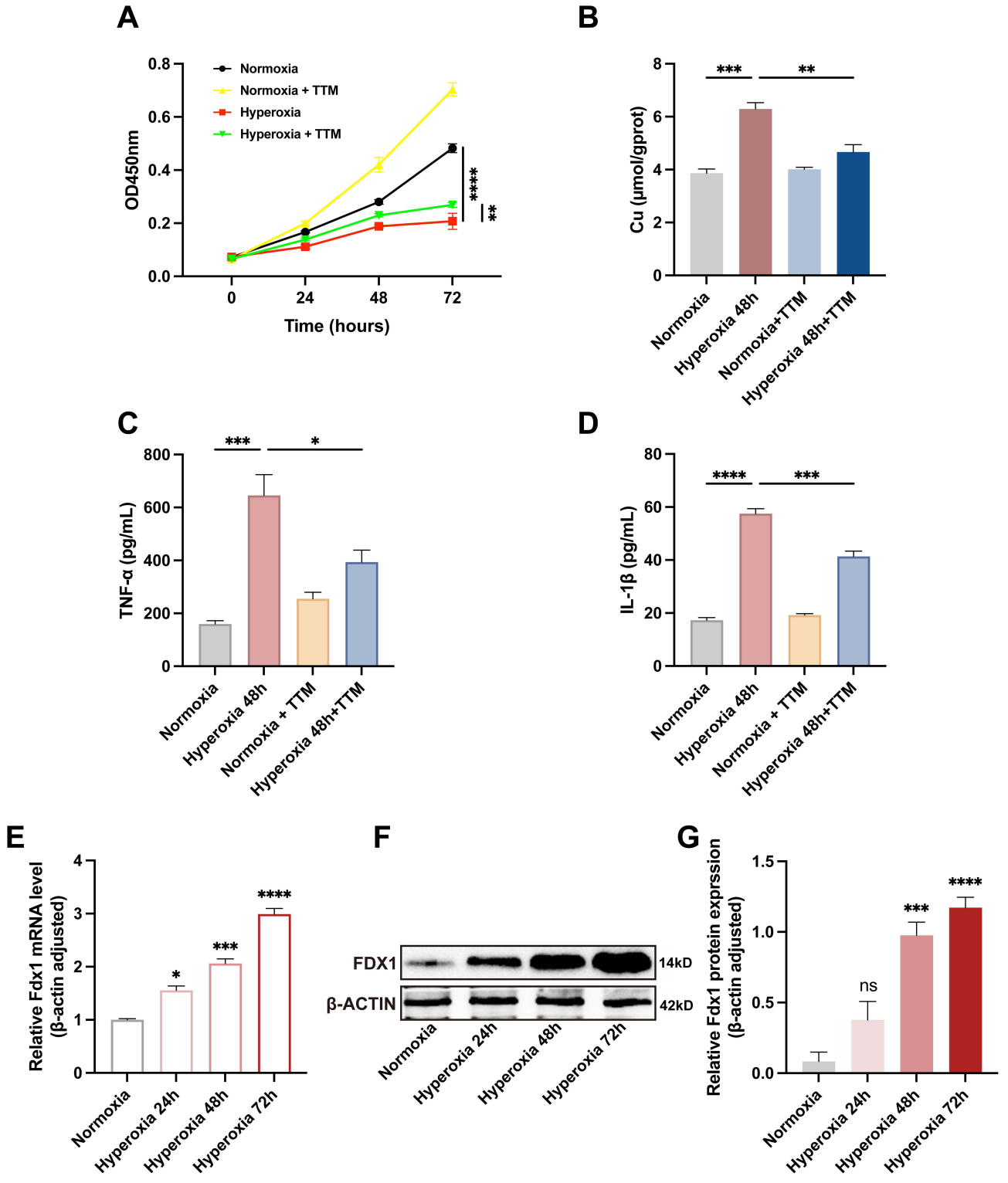

Figure 2 The copper chelator TTM attenuates hyperoxia-induced injury, reduces intracellular copper content, and upregulates the cuproptosis-related gene *Fdx1* in MLE-12 cells. (**A**) Cell proliferation quantified by CCK-8 assay. (**B**) Copper concentration within cells. (**C**) TNF-α levels in culture supernatants. (**D**) IL-1β levels in culture supernatants. (**E**) Quantitative reverse transcription PCR analysis of *Fdx1* in cells. (**F**) Western blot analysis of FDX1 in cells. (**G**) Densitometric analysis of FDX1 in cells. The data were expressed as mean ± SEM, n = 3. **P*<0.05, ***P*<0.01, ****P*<0.001, *****P*< 0.0001 versus normoxia group.

observed in the Hyperoxia group compared to the Normoxia group, all of which were effectively reduced by TTM treatment (Figure 4B–D). The wet/dry weight ratio was significantly increased in the Hyperoxia group but was decreased with TTM treatment (Figure 4E). Total cell count and protein concentration in BALF were also significantly elevated in

the Hyperoxia group, but both decreased following TTM treatment (Figure 4F and G). To further assess the anti-inflammatory effects of TTM, ELISA was performed to measure TNF-α and IL-1β levels in BALF. These pro-inflammatory cytokines were elevated after hyperoxia exposure but reduced with TTM treatment (Figure 4H and I). Moreover, copper levels in serum and lung tissues were significantly increased under hyperoxia but decreased with TTM treatment (Figure 4J and K). Mice in the Hyperoxia group showed slower weight gain, which was partially improved by TTM treatment (Figure 4L). In summary, these findings indicate that hyperoxia induces lung inflammation, while TTM exhibits anti-inflammatory effects, suggesting that cuproptosis may be involved in this process.

Cuproptosis Involved in Hyperoxia-Induced Lung Injury in Mice

To determine whether hyperoxia induces cuproptosis in a manner similar to that observed in MLE-12 cells, we assessed the expression of cuproptosis-related genes in lung tissue using qRT-PCR (Figure 5A–M). Under hyperoxic conditions, mRNA levels of *Fdx1, Lias, Lipt1, Dld, Gls, Mtf1, Cdkn2a, Slc31a1, Atp7b*, and *Hsp70* were significantly upregulated, while *Pdha1* and *Pdhb* were notably downregulated, compared to the normoxic controls. Treatment with TTM for 7 days effectively reversed these gene expression changes. At the protein level, FDX1 and SLC31A1 showed similar trends.

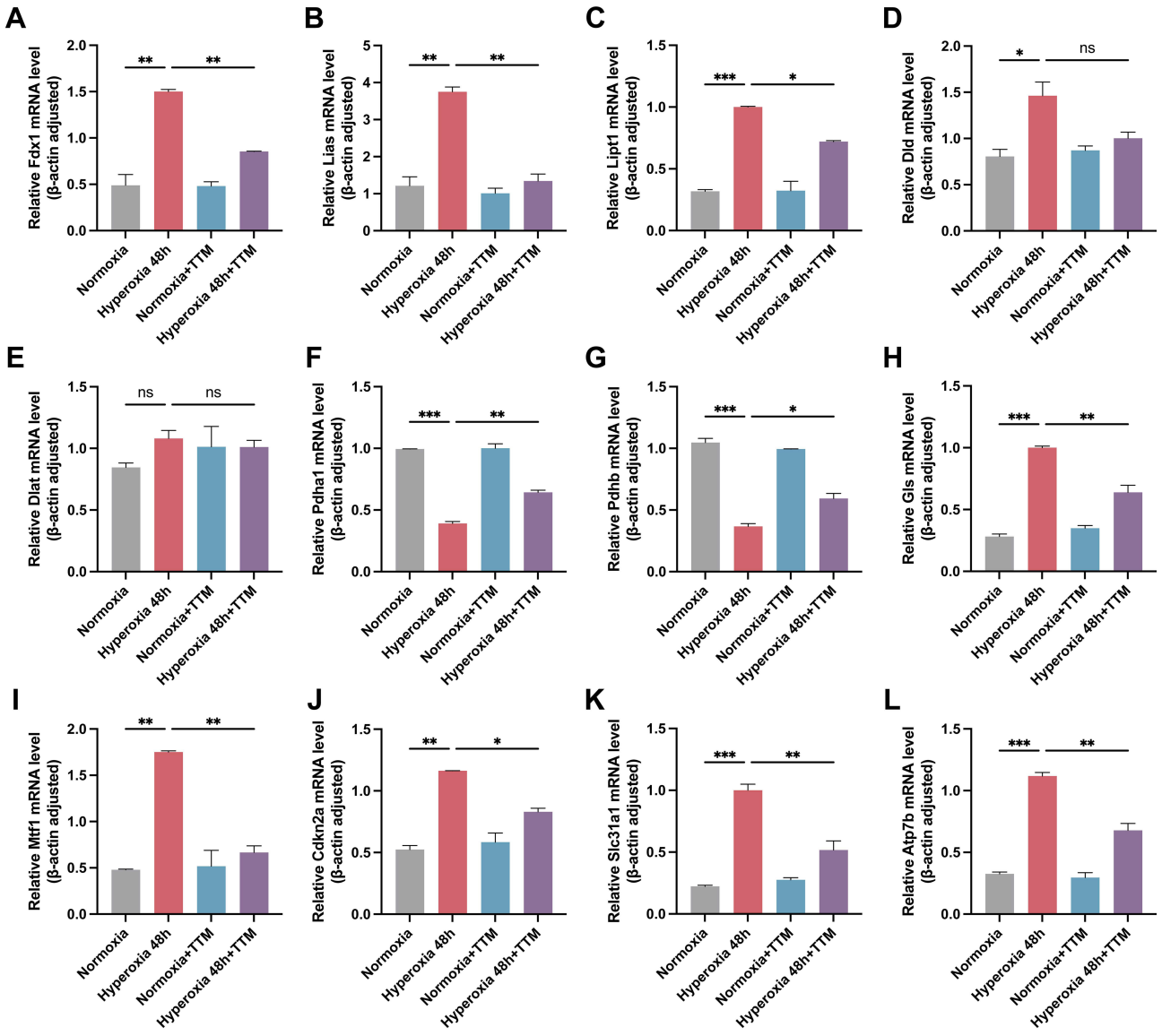

Figure 3 Continued.

https://doi.org/10.2147/JIR.S512187

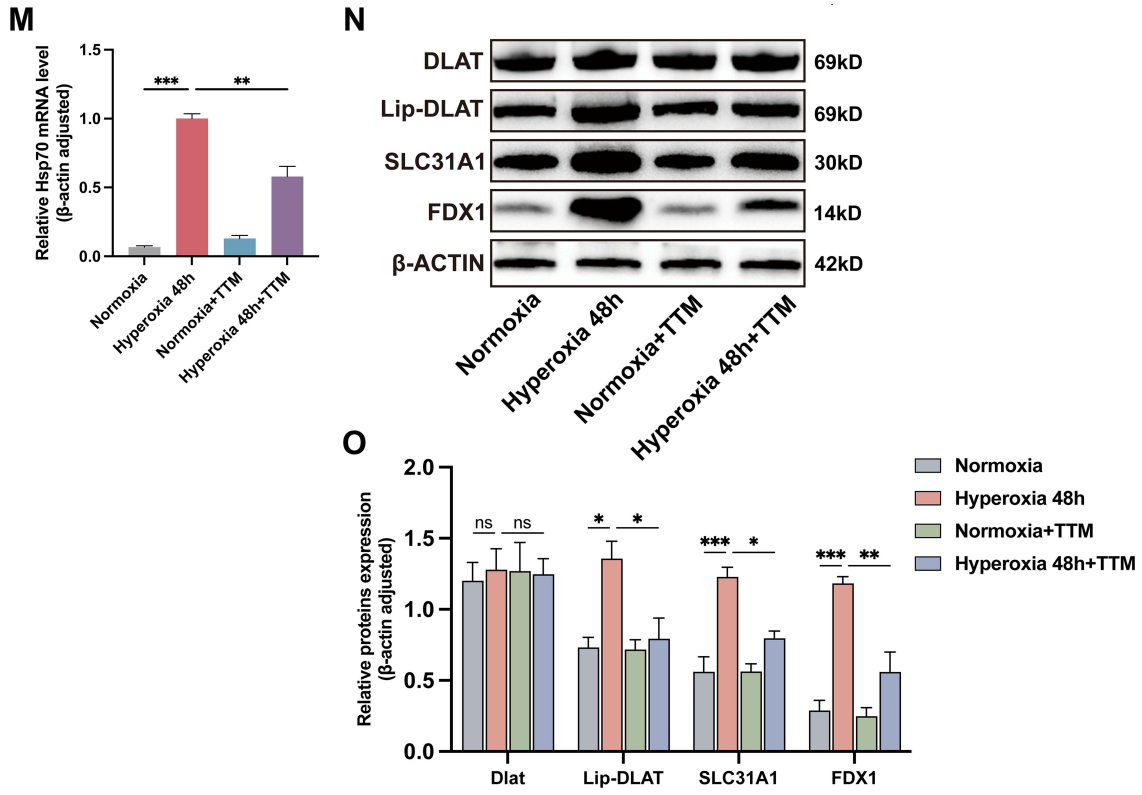

Figure 3 Effects of hyperoxia on the expression of cuproptosis-related genes and proteins in MLE-12 cells. (**A-M**) Quantitative reverse transcription PCR analysis of cuproptosis-related genes: *Fdx1*, *Lias*, *Lipt1*, *Dld*, *Dlat*, *Pdha1*, *Pdhb*, *Gls*, *Mtf1*, *Cdkn2a*, *Slc31a1*, *Atp7b*, and *Hsp70* in cells. (**N**) Western blot analysis of DLAT, Lip-DLAT, SLC31A1, FDX1 in cells. (**O**) Densitometric analysis of DLAT, Lip-DLAT, SLC31A1, and FDX1 in cells. The data were expressed as mean ± SEM, n = 3. **P*<0.05, ***P*<0.01, ****P*<0.001.

Although hyperoxia did not affect *Dlat* mRNA and protein levels, it significantly increased the protein level of lipoylated-DLAT, which was markedly reduced by TTM treatment (Figure 5N and O).

Discussion

Hyperoxia is commonly administered in various medical settings, but excessive oxygen exposure can lead to adverse outcomes, including increased mortality and lung injury characterized by disrupted mechanics and inflammation.[18–20] Despite extensive research, the molecular mechanisms underlying HLI remain unclear. This study is the first to explore the potential role of cuproptosis in the development of HLI. Our findings demonstrated that hyperoxia significantly increased copper levels in MLE-12 cells, as well as in the lung tissue and serum of mice. Notably, a recent study showed that copper accumulation disrupted mitochondrial respiration through the TCA cycle and induces cuproptosis.[9] Previous research has implicated cuproptosis in the pathogenesis of various lung diseases, such as bronchopulmonary dysplasia, idiopathic pulmonary fibrosis, and lung cancer.[21–25] Therefore, we aimed to verify whether this novel form of cell death is involved in the pathogenesis of HLI.

Moreover, our analysis revealed a marked upregulation of both mRNA and protein levels of the copper importer SLC31A1 following hyperoxia exposure, indicating that hyperoxia may promote copper accumulation and lead to copper overload. As a critical copper transport protein, SLC31A1 plays a pivotal role in maintaining cellular copper homeostasis. We speculate that the increased expression of SLC31A1 observed in this study contributes to the copper overload during HLI.

To determine whether cuproptosis is involved in HLI, we examined *Fdx1* expression levels through qRT-PCR and Western blot. Our results demonstrated a significant, time-dependent increase in *Fdx1* mRNA and protein expression under prolonged hyperoxia, compared to the normoxic conditions. FDX1, a mitochondrial reductase, reduces Cu^{2+} to its

more toxic form, Cu^{1+}, thereby participating in various biosynthetic pathways.[26] Moreover, FDX1 acts as an upstream regulator of DLAT lipoylation, which is essential for cuproptosis. It is also a direct target of the copper ionophore elesclomol.[27] Notably, knocking out FDX1 partially shields cells from copper-induced toxicity, suggesting its involvement in copper-related cell damage. In contrast, increased copper levels in wild-type cells and copper toxicity models led to reduced protein levels of FDX1, DLAT, and lipoylated DLAT, indicating that elevated copper levels may downregulate FDX1 and provide a protective effect against copper toxicity.[9] This creates a contradictory relationship, where FDX1 is

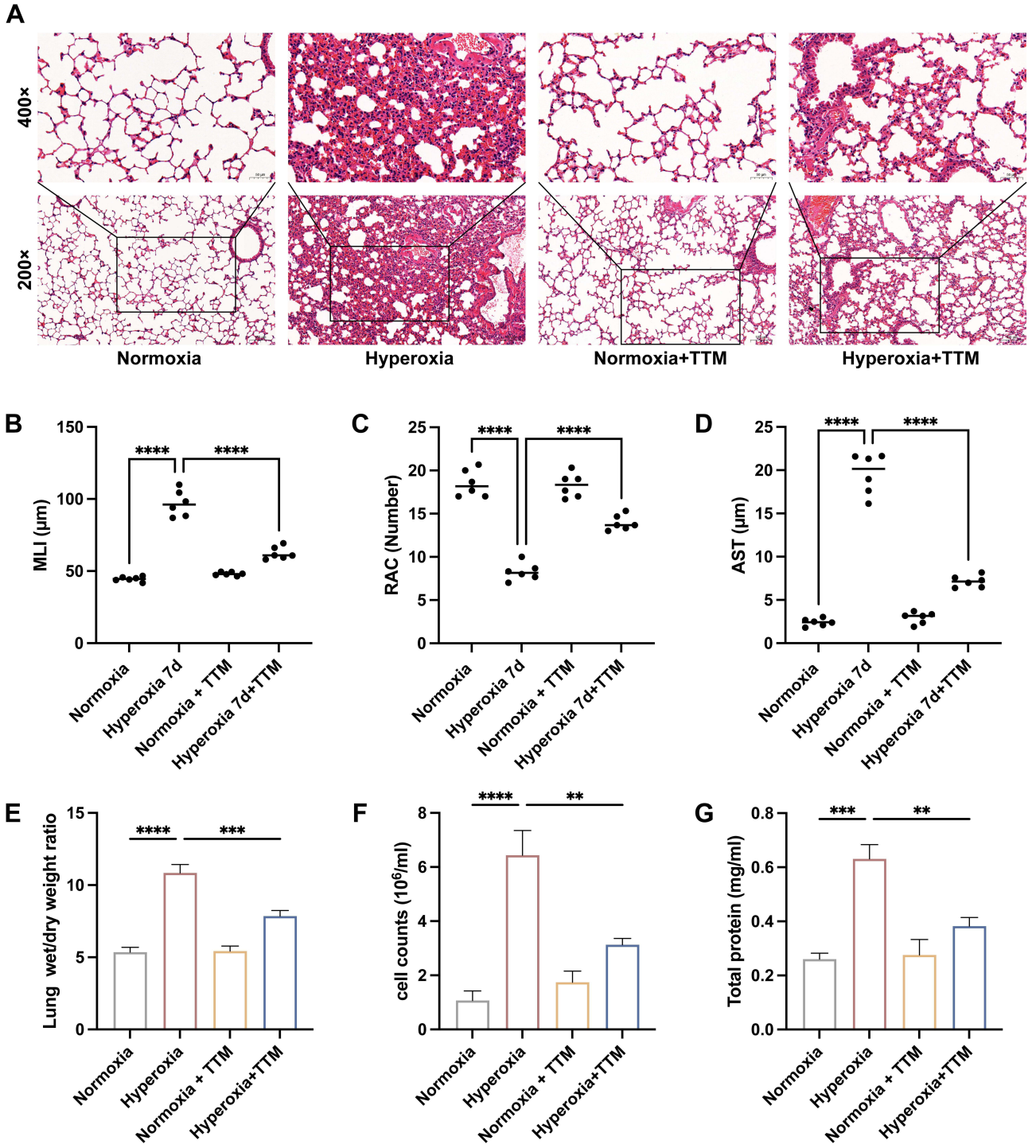

Figure 4 Continued.

https://doi.org/10.2147/JIR.S512187

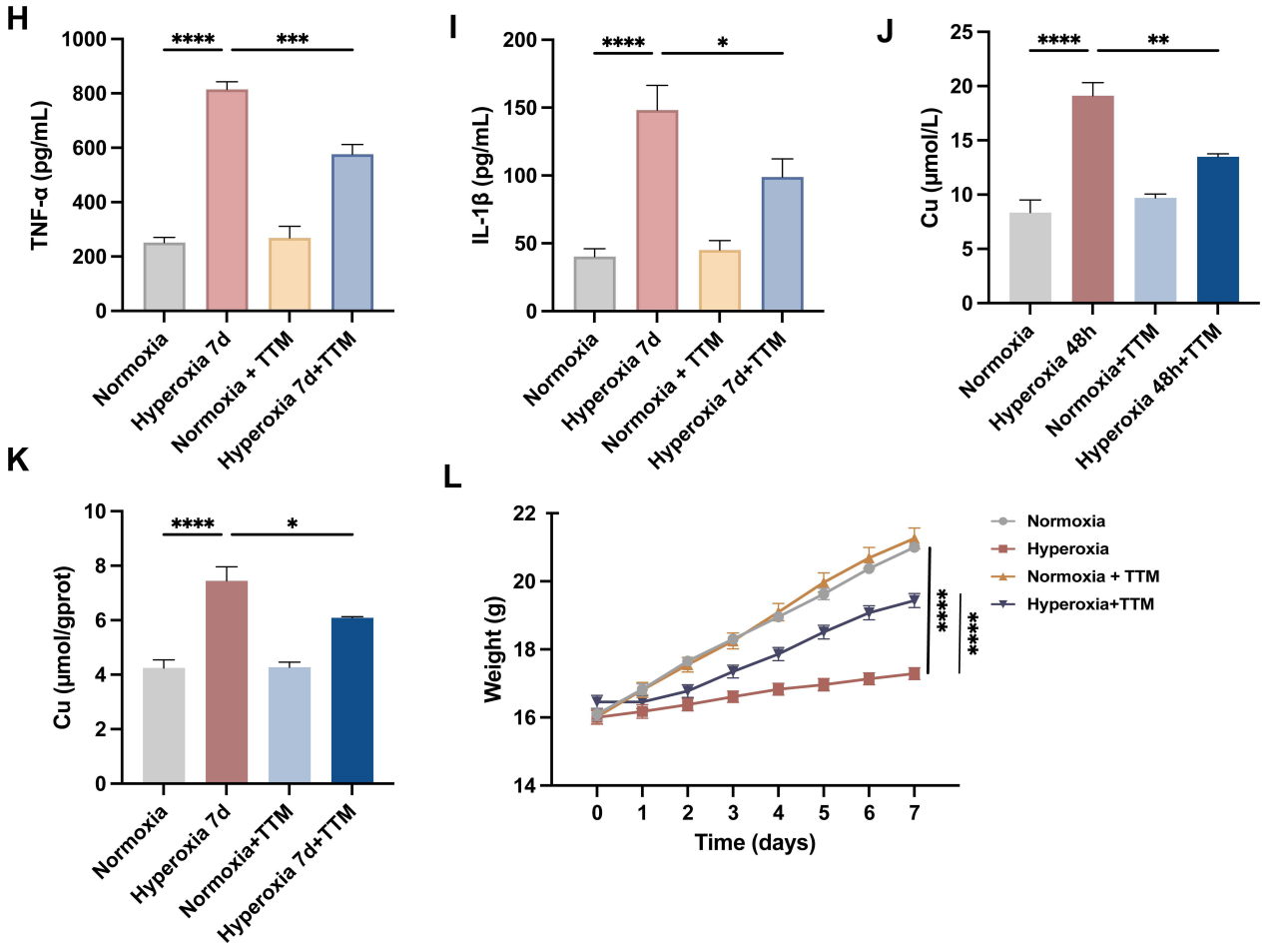

Figure 4 The copper inhibitor TTM attenuates lung injury, decreases copper content, and improves growth in C57BL/6 mice under hyperoxic conditions. (**A**) Histopathological changes in lung tissue (upper: ×400; scale bar, 50 μm; lower: ×200; scale bar, 100 μm). (**B**) Semi-quantitative pathology score of MLI in lung tissue. (**C**) Semi-quantitative pathology score of RAC in lung tissue. (**D**) Semi-quantitative pathology score of AST in lung tissue. (**E**) Lung wet/dry weight ratio. (**F**) Total cell count in BALF. (**G**) Total protein concentration in BALF. (**H**) Levels of TNF-α in BALF. (**I**) Levels of IL-1β in BALF. (**J**) The concentrations of copper in serum. (**K**) The concentrations of copper in lung tissue. (**L**) Body weight changes.The data were expressed as mean ± SEM, n =6. **P*<0.05, ***P*<0.01, ****P*<0.001, *****P*< 0.0001.

involved in promoting cell death under certain conditions, while its reduction may lead to enhanced cell survival under high copper exposure. Thus, it is worthwhile to delve into the role of FDX1 in various disease models.

In our study, hyperoxia did not affect DLAT protein levels but significantly increased lipoylated DLAT levels in the hyperoxia group. These findings are consistent with a recent study in a chicken liver model, which also observed elevated lipoylated DLAT levels under natural copper stress, without changes in DLAT levels.[28] While our findings differ in certain aspects from previous studies, they underscore that the specific mechanisms of cuproptosis are influenced by various factors.

Genes associated with cuproptosis include *Fdx1, Lias, Lipt1, Dld, Dlat, Pdha1, Pdhb, Gls, Mtf1*, and *Cdkn2a*. Among these genes, *Lias, Lipt1*, and *Dld* are associated with the lipoic acid pathway, while *Dlat, Pdha1*, and *Pdhb* are components of the pyruvate dehydrogenase (PDH) complex. The lipoic acid pathway and the PDH complex both play essential roles in the regulation of cuproptosis.[9] Lipoic acid, an organosulfur compound derived from caprylic acid, serves as an essential cofactor for several mitochondrial multi-enzyme complexes that facilitate aerobic metabolism.[27] Its robust antioxidant capabilities help counteract reactive oxygen species and support other antioxidants.[29] These features make it a potential treatment for oxidative stress-related conditions, such as atherosclerosis, diabetes, neurodegenerative disorders, and heavy metal toxicity.[30–33] The PDH complex oxidizes pyruvate to acetyl-CoA, providing substrate for the TCA cycle and facilitating cellular energy production from glycolysis.[34] Studies have shown that disruptions in PDH metabolism can elicit oxidative stress.[35,36]

GLS is an enzyme responsible for converting glutamine to glutamate. Glutamate serves as a substrate for GSH synthesis, which helps neutralize free radicals and peroxides, thereby maintaining redox balance.[37,38] The study showed that hyperoxia induced glutamine-fueled anaplerosis, shifting metabolic flux from glutamine biosynthesis to its utilization.[39] MTF1 maintains intracellular metal homeostasis and mitigates oxidative stress by binding to metal-responsive elements and modulating gene expression in response to fluctuations in metal concentrations.[40] MTF1 interacts with diverse metals, including Zn, Cu, and Cd, and plays a critical role in processes such as myogenesis, embryonic liver development, and heavy metal detoxification in the adult liver.[41,42] Additionally, MTF1 regulates apoptosis and tumor development.[43,44] Beyond metal regulation, MTF1 enhances antioxidant enzyme expression, mitigates oxidative damage, and modulates autophagy, inflammation, and other signaling pathways to maintain cellular homeostasis.[40,45,46] Specifically, under high copper conditions, MTF1 activates metallothioneins to safeguard cells from copper-induced toxicity.[47]

CDKN2A encodes two tumor suppressor proteins, p16 and p14, both of which are critical regulators of the cell cycle. A previous study reported that p16 knockout mice, when fed a pro-steatotic diet, exhibited more severe liver lipid deposition, inflammation, and ROS accumulation than wild-type mice.[48] Our qRT-PCR analysis revealed altered mRNA expression profiles of multiple genes associated with cuproptosis following hyperoxia exposure. These data suggest that

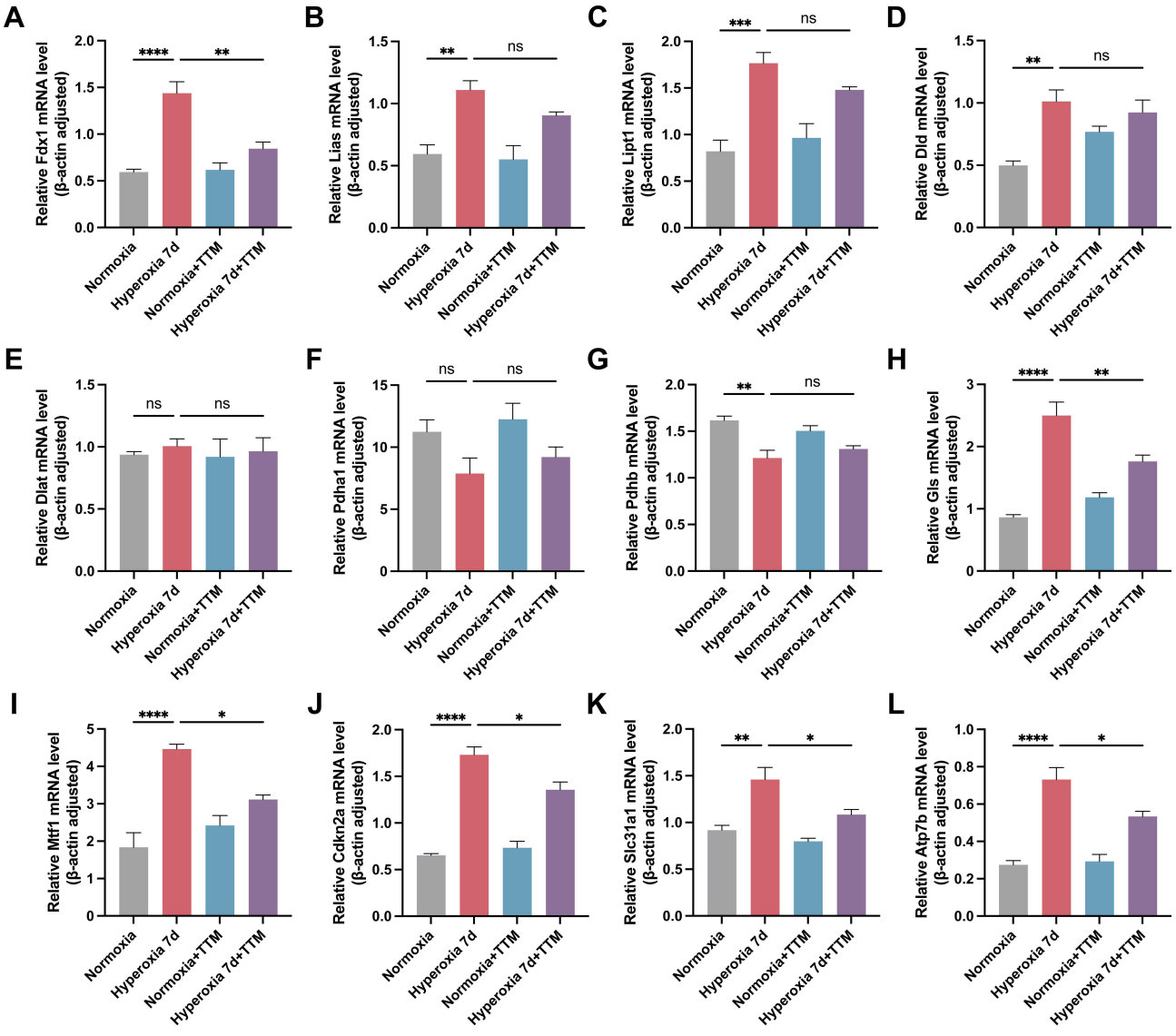

Figure 5 Continued.

https://doi.org/10.2147/JIR.S512187

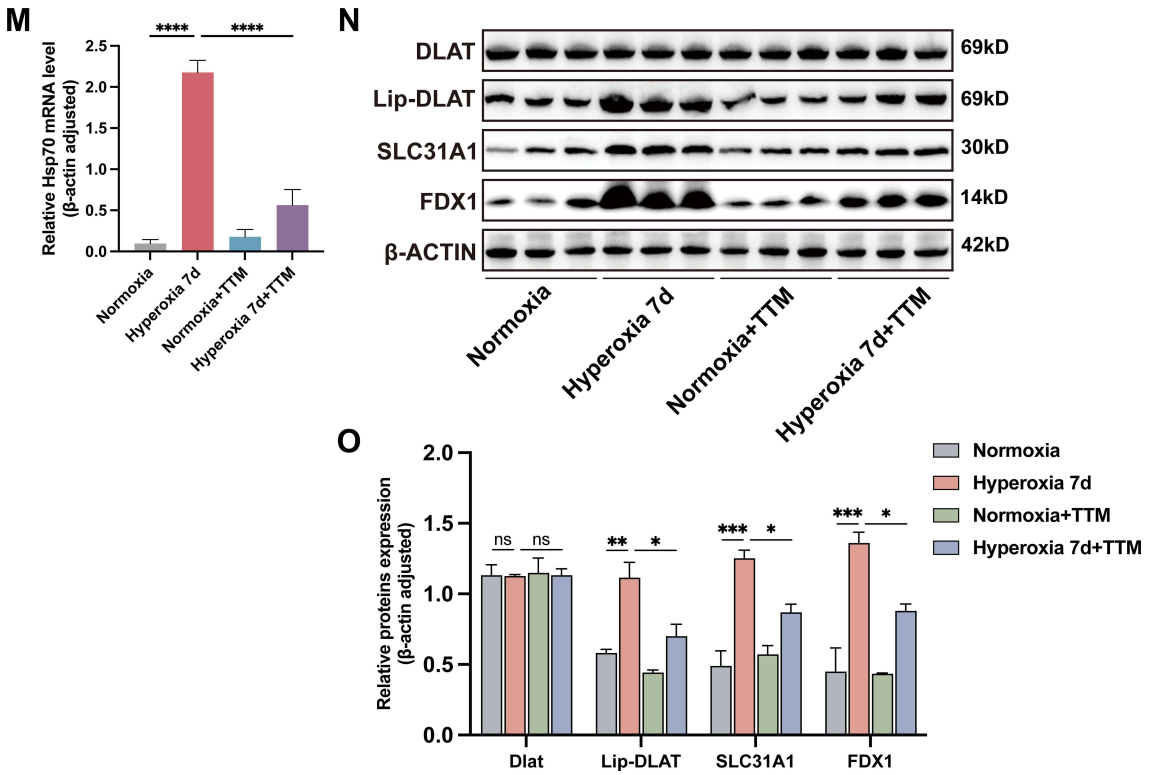

Figure 5 Effects of hyperoxia on the expression of cuproptosis-related genes and proteins in C57BL/6 mice. (**A-M**) Quantitative reverse transcription PCR analysis of cuproptosis-related genes: *Fdx1*, *Lias*, *Lipt1*, *Dld*, *Dlat*, *Pdha1*, *Pdhb*, *Gls*, *Mtf1*, *Cdkn2a*, *Slc31a1*, *Atp7b*, and *Hsp70* in lung tissue. (**N**) Western blot analysis of DLAT, Lip-DLAT, SLC31A1, FDX1 in lung tissue. (**O**) Densitometric analysis of DLAT, Lip-DLAT, SLC31A1, and FDX1 in lung tissue. The data were expressed as mean ± SEM, n = 6. **P*<0.05, ***P*<0.01, ****P*<0.001, *****P*< 0.0001.

hyperoxia may trigger cuproptosis in cultured MLE-12 cells and mouse lung tissue. Conversely, treatment with TTM effectively mitigated the severity of hyperoxia-induced injury. In conjunction with these results, our findings confirmed that *Fdx1*-mediated protein lipoylation and the resulting proteotoxic stress play a pivotal role in the pathogenesis of HLI.

Our findings indicate that targeting cuproptosis could serve as a promising therapeutic approach for treating HLI. While this study establishes the role of cuproptosis in HLI and highlights the protective effects of TTM, it also raises several critical questions that remain unanswered: (1) While this study focused on cuproptosis, the potential involvement of other cell death pathways in HLI has not been explored. (2) Although the association between cuproptosis and HLI has been established, the precise mechanisms underlying cuproptosis in HLI still need further investigation, particularly the role of MTF1 in this process, which remains unclear. (3) Since all experiments were conducted in cell lines, it is crucial to conduct further studies using primary cells to validate these findings. (4) The role of mitochondrial homeostasis in cuproptosis under hyperoxia remains unclear. The PDH complex, a key component of mitochondrial energy metabolism, may influence oxidative stress and cuproptosis, with the exact mechanisms requiring further investigation. Addressing these questions will deepen our understanding of the role of cuproptosis in the pathogenesis of HLI.

Conclusion

In conclusion, this study is the first to confirm that hyperoxia-induced cuproptosis represents a potential novel mechanism underlying HLI. Our findings demonstrate that hyperoxia upregulates the copper importer SLC31A1, which leads to copper accumulation, disrupts copper homeostasis, and promotes cuproptosis. Moreover, hyperoxia alters the expression of genes associated with cuproptosis. Conversely, TTM administration reverses these changes and provides protective effects against hyperoxia-induced injury in both MLE-12 cells and mouse lung tissue. However, further studies are needed to clarify the precise role of cuproptosis in HLI. In summary, cuproptosis plays a pivotal role in HLI pathogenesis, and targeting this pathway may represent a promising therapeutic strategy.

Abbreviations

HLI, hyperoxia-induced lung injury; ROS, reactive oxygen species; TCA, tricarboxylic acid; GSH, glutathione; CYP, Cytochrome P450; DMEM, dulbecco's modified eagle medium; TTM, tetrathiomolybdate; PDH, pyruvate dehydrogenase.

Data Sharing Statement

The data supporting this study's findings are available from the corresponding author upon reasonable request.

Funding

This work was supported by the Natural Science Foundation of Gansu Province[21 JR1RA062].

Disclosure

The authors declare that there are no competing interests associated with the manuscript.

References

1. Angus DC. Oxygen therapy for the critically ill. *N Engl J Med*. 2020;382(11):1054–1056. doi:10.1056/NEJMe2000800
2. Simonis FD, Juffermans NP, Schultz MJ. Mechanical ventilation of the healthy lungs: lessons learned from recent trials. *Curr Opin Crit Care*. 2021;27(1):55–59. doi:10.1097/mcc.0000000000000787
3. Schmidt-Rohr K. Oxygen is the high-energy molecule powering complex multicellular life: fundamental corrections to traditional bioenergetics. *ACS Omega*. 2020;5(5):2221–2233. doi:10.1021/acsomega.9b03352
4. Barazzone C, Horowitz S, Donati YR, Rodriguez I, Piguet PF. Oxygen toxicity in mouse lung: pathways to cell death. *Am J Respir Cell mol Biol*. 1998;19(4):573–581. doi:10.1165/ajrcmb.19.4.3173
5. Ruaro B, Salton F, Braga L, et al. The history and mystery of alveolar epithelial type ii cells: focus on their physiologic and pathologic role in lung. *Int J mol Sci*. 2021;22(5). doi:10.3390/ijms22052566
6. Wang Y, Wang L, Ma S, Cheng L, Yu G. Repair and regeneration of the alveolar epithelium in lung injury. *FASEB j*. 2024;38(8):e23612. doi:10.1096/fj.202400088R
7. Zhang L, Zhao S, Yuan LJ, et al. Autophagy regulates hyperoxia-induced intracellular accumulation of surfactant protein C in alveolar type II cells. *mol Cell Biochem*. 2015;408(1–2):181–189. doi:10.1007/s11010-015-2494-z
8. Sakurai T, Kataoka K. Structure and function of type I copper in multicopper oxidases. *Cell mol Life Sci*. 2007;64(19–20):2642–2656. doi:10.1007/s00018-007-7183-y
9. Tsvetkov P, Coy S, Petrova B, et al. Copper induces cell death by targeting lipoylated TCA cycle proteins. *Science*. 2022;375(6586):1254–1261. doi:10.1126/science.abf0529
10. Kelly KA, Havrilla CM, Brady TC, Abramo KH, Levin ED. Oxidative stress in toxicology: established mammalian and emerging piscine model systems. *Environ Health Perspect*. 1998;106(7):375–384. doi:10.1289/ehp.98106375
11. Tsang T, Davis CI, Brady DC. Copper biology. *Curr Biol*. 2021;31(9):R421–r427. doi:10.1016/j.cub.2021.03.054
12. Speisky H, Gómez M, Burgos-Bravo F, et al. Generation of superoxide radicals by copper-glutathione complexes: redox-consequences associated with their interaction with reduced glutathione. *Bioorg Med Chem*. 2009;17(5):1803–1810. doi:10.1016/j.bmc.2009.01.069
13. Robbins ME, Cho HY, Hansen JM, et al. Glutathione reductase deficiency alters lung development and hyperoxic responses in neonatal mice. *Redox Biol*. 2021;38:101797. doi:10.1016/j.redox.2020.101797
14. Zangar RC, Davydov DR, Verma S. Mechanisms that regulate production of reactive oxygen species by cytochrome P450. *Toxicol Appl Pharmacol*. 2004;199(3):316–331. doi:10.1016/j.taap.2004.01.018
15. Hanukoglu I, Jefcoate CR. Mitochondrial cytochrome P-450scc. mechanism of electron transport by adrenodoxin. *J Biol Chem*. 1980;255(7):3057–3061. doi:10.1016/s0021-9258(19)85851-9
16. Grimm SL, Stading RE, Robertson MJ, et al. Loss of cytochrome P450 (CYP)1B1 mitigates hyperoxia response in adult mouse lung by reprogramming metabolism and translation. *Redox Biol*. 2023;64:102790. doi:10.1016/j.redox.2023.102790
17. Baik AH, Haribowo AG, Chen X, et al. Oxygen toxicity causes cyclic damage by destabilizing specific Fe-S cluster-containing protein complexes. *Mol Cell*. 2023;83(6):942–960.e9. doi:10.1016/j.molcel.2023.02.013
18. Aggarwal NR, D'Alessio FR, Tsushima K, et al. Moderate oxygen augments lipopolysaccharide-induced lung injury in mice. *Am J Physiol Lung Cell mol Physiol*. 2010;298(3):L371–81. doi:10.1152/ajplung.00308.2009
19. Hanidziar D, Robson SC. Hyperoxia and modulation of pulmonary vascular and immune responses in COVID-19. *Am J Physiol Lung Cell mol Physiol*. 320(1):L12–l16. doi:10.1152/ajplung.00304.2020
20. Narala VR, Thimmana LV, Panati K, Kolliputi N. Nitrated fatty acid, 10-nitrooleate protects against hyperoxia-induced acute lung injury in mice. *Int Immunopharmacol*. 2022;109:108838. doi:10.1016/j.intimp.2022.108838
21. Zhang W, Qu H, Ma X, et al. Identification of cuproptosis and immune-related gene prognostic signature in lung adenocarcinoma. *Front Immunol*. 2023;14:1179742. doi:10.3389/fimmu.2023.1179742
22. Qi W, Liu L, Zeng Q, et al. Contribution of cuproptosis and Cu metabolism-associated genes to chronic obstructive pulmonary disease. *J Cell Mol Med*. 2023;27(24):4034–4044. doi:10.1111/jcmm.17985
23. Qin J, Xiao X, Li S, et al. Identification of cuproptosis-related biomarkers and analysis of immune infiltration in allograft lung ischemia-reperfusion injury. *Front Mol Biosci*. 2023;10:1269478. doi:10.3389/fmolb.2023.1269478

24. Xu B, Yang K, Han X, Hou J. Cuproptosis-related gene CDKN2A as a molecular target for IPF diagnosis and therapeutics. *Inflamm Res*. 2023;72(6):1147–1160. doi:10.1007/s00011-023-01739-7
25. Jia M, Li J, Zhang J, et al. Identification and validation of cuproptosis related genes and signature markers in bronchopulmonary dysplasia disease using bioinformatics analysis and machine learning. *BMC Med Inform Decis Mak*. 2023;23(1):69. doi:10.1186/s12911-023-02163-x
26. Tsvetkov P, Detappe A, Cai K, et al. Mitochondrial metabolism promotes adaptation to proteotoxic stress. *Nat Chem Biol*. 2019;15(7):681–689. doi:10.1038/s41589-019-0291-9
27. Solmonson A, DeBerardinis RJ. Lipoic acid metabolism and mitochondrial redox regulation. *J Biol Chem*. 2018;293(20):7522–7530. doi:10.1074/jbc.TM117.000259
28. Zhong G, Li L, Li Y, et al. Cuproptosis is involved in copper-induced hepatotoxicity in chickens. *Sci Total Environ*. 2023;866:161458. doi:10.1016/j.scitotenv.2023.161458
29. Salehi B, Berkay Yılmaz Y, Antika G, et al. Insights on the Use of α-Lipoic Acid for Therapeutic Purposes. *Biomolecules*. 9(8). doi:10.3390/biom9080356
30. Lu X, He Z, Xiao X, Wei X, Song X, Zhang S. Natural antioxidant-based nanodrug for atherosclerosis treatment. *Small*. 2023;19(49):e2303459. doi:10.1002/smll.202303459
31. Henriksen EJ. Exercise training and the antioxidant alpha-lipoic acid in the treatment of insulin resistance and type 2 diabetes. *Free Radic Biol Med*. 2006;40(1):3–12. doi:10.1016/j.freeradbiomed.2005.04.002
32. Tóth F, Cseh EK, Vécsei L. natural molecules and neuroprotection: kynurenic acid, pantethine and α-lipoic acid. *Int J mol Sci*. 22(1). doi:10.3390/ijms22010403
33. Ciftci H, Bakal U. The effect of lipoic acid on macro and trace metal levels in living tissues exposed to oxidative stress. *Anticancer Agents Med Chem*. 2009;9(5):560–568. doi:10.2174/187152009788451815
34. Chalifoux O, Faerman B, Mailloux RJ. Mitochondrial hydrogen peroxide production by pyruvate dehydrogenase and α-ketoglutarate dehydrogenase in oxidative eustress and oxidative distress. *J Biol Chem*. 2023;299(12):105399. doi:10.1016/j.jbc.2023.105399
35. Starkov AA, Fiskum G, Chinopoulos C, et al. Mitochondrial alpha-ketoglutarate dehydrogenase complex generates reactive oxygen species. *J Neurosci*. 2004;24(36):7779–7788. doi:10.1523/jneurosci.1899-04.2004
36. Tretter L, Adam-Vizi V. Generation of reactive oxygen species in the reaction catalyzed by alpha-ketoglutarate dehydrogenase. *J Neurosci*. 2004;24(36):7771–7778. doi:10.1523/jneurosci.1842-04.2004
37. Le A, Lane AN, Hamaker M, et al. Glucose-independent glutamine metabolism via TCA cycling for proliferation and survival in B cells. *Cell Metab*. 2012;15(1):110–121. doi:10.1016/j.cmet.2011.12.009
38. Mukha A, Kahya U, Linge A, et al. GLS-driven glutamine catabolism contributes to prostate cancer radiosensitivity by regulating the redox state, stemness and ATG5-mediated autophagy. *Theranostics*. 2021;11(16):7844–7868. doi:10.7150/thno.58655
39. Singh C, Tran V, McCollum L, et al. Hyperoxia induces glutamine-fuelled anaplerosis in retinal Müller cells. *Nat Commun*. 2020;11(1):1277. doi:10.1038/s41467-020-15066-6
40. Giedroc DP, Chen X, Apuy JL. Metal response element (MRE)-binding transcription factor-1 (MTF-1): structure, function, and regulation. *Antioxid Redox Signal*. 2001;3(4):577–596. doi:10.1089/15230860152542943
41. Wang Y, Wimmer U, Lichtlen P, et al. Metal-responsive transcription factor-1 (MTF-1) is essential for embryonic liver development and heavy metal detoxification in the adult liver. *FASEB j*. 2004;18(10):1071–1079. doi:10.1096/fj.03-1282com
42. Tavera-Montañez C, Hainer SJ, Cangussu D, et al. The classic metal-sensing transcription factor MTF1 promotes myogenesis in response to copper. *FASEB j*. 2019;33(12):14556–14574. doi:10.1096/fj.201901606R
43. Hübner C, Haase H. Interactions of zinc- and redox-signaling pathways. *Redox Biol*. 2021;41:101916. doi:10.1016/j.redox.2021.101916
44. Cheng Y, Zhang C, Li Q, et al. MTF1 genetic variants are associated with lung cancer risk in the Chinese Han population. *BMC Cancer*. 2024;24(1):778. doi:10.1186/s12885-024-12516-y
45. Kim HG, Huang M, Xin Y, et al. The epigenetic regulator SIRT6 protects the liver from alcohol-induced tissue injury by reducing oxidative stress in mice. *J Hepatol*. 2019;71(5):960–969. doi:10.1016/j.jhep.2019.06.019
46. Xiong T, Li Y, Yang M, et al. Metallothionein 3 potentiates pulmonary artery smooth muscle cell proliferation by promoting zinc-MTF1-ATG5 axis-mediated autophagosome formation. *Int J Biol Sci*. 2024;20(8):2904–2921. doi:10.7150/ijbs.92992
47. Balamurugan K, Schaffner W. Copper homeostasis in eukaryotes: teetering on a tightrope. *Biochim Biophys Acta*. 2006;1763(7):737–746. doi:10.1016/j.bbamcr.2006.05.001
48. Lv F, Li N, Kong M, et al. CDKN2a/p16 antagonizes hepatic stellate cell activation and liver fibrosis by modulating ROS levels. *Front Cell Dev Biol*. 2020;8:176. doi:10.3389/fcell.2020.00176